Title for citationTitle for citation

SCIENCE CHINA
Information Sciences

• Supplementary File •

Wideband Chaos Generation Using a VCSEL With Intensity Modulation Optical Injection for Random Number Generation

Yu HUANG[1], Shuangquan GU[1], Yuhang FENG[1], Yigong YANG[1], Shuiying XIANG[3], Pei ZHOU[1] & Nianqiang LI[1,2*]

[1]*School of Optoelectronic Science and Engineering & Collaborative Innovation Center of Suzhou Nano Science and Technology, Soochow University, Suzhou* 215006*, China;*
[2]*Key Lab of Advanced Optical Manufacturing Technologies of Jiangsu Province & Key Lab of Modern Optical Technologies of Education Ministry of China, Soochow University, Suzhou* 215006*, China;*
[3]*State Key Laboratory of Integrated Service Networks, Xidian University, Xi'an* 710071*, China*

Appendix A Introduction

Random numbers have been widely used in modern network society, such as the generation of cryptographic keys for classical and quantum cryptography systems [1-4]. Early, random numbers can be generated using deterministic algorithm programs, called pseudorandom numbers, which show limited unpredictability and thus reduce the randomness and security [5]. To overcome this flaw, physical entropy sources have been proposed to yield the random number, e.g., electronic and photon noises, random optoelectronic oscillators [6], thermal noises in resistors [7], and semiconductor lasers [8-11]. Among them, chaotic semiconductor lasers have many desired characteristics (including larger bandwidth, low cost, and monolithic integration) and have thus attracted wide attention in the generation of random numbers [12], chaotic lidar/radar [13], and secure communications [14, 15]. In the last decade, a variety of semiconductor lasers have been proposed to gain high-quality chaos signals, such as distributed-feedback (DFB) semiconductor lasers [16-18], semiconductor ring lasers [19, 20], quantum dot lasers [21], microcavity lasers [22], interband cascade lasers [23], Fabry-Perot lasers [24, 25], and (spin) vertical-cavity surface-emitting lasers (VCSELs) [26, 27]. In particular, VCSELs have the advantages of low threshold current, small size, and easy integration into large-scale arrays and are thus regarded as excellent candidates for chaos generation.

In recent years, the chaos signal generation scheme based on VCSELs can be summarized into two kinds. On the one hand, Virte et al. experimentally demonstrated that a free-running VCSEL presents polarization chaos dynamics, which originates from a nonlinear coupling between two elliptically polarized modes [25]. Adams and Li et al. found that VCSELs can produce polarization chaos dynamics in a wide parameter range by injecting the spin carrier into the active region, which is called spin-VCSELs [26, 28-31]. Although these schemes can generate chaotic signals only using a single structure (a solitary VCSEL), the chaotic bandwidth and dimension are limited, which is unbeneficial to practical applications. On the other hand, by introducing the external perturbation (i.e., optical feedback or injection), polarization chaos can be observed in VCSELs. For example, Priyadarshi and Hong et al. proposed and experimentally demonstrated a chaos signal in VCSELs with polarization optical feedback [32-34]. Inevitably, the introduction of an external cavity causes chaos signals with a weak periodicity, which has been termed time-delay signature (TDS). In their work, TDS can be suppressed by controlling key parameters, such as the optical polarization angle of feedback and feedback strength. Moreover, some post-processing methods have been proposed to suppress TDS, such as using a fiber ring resonator [35]. Xia and Xiang et al. also demonstrated that the fiber Bragg grating feedback employed in VCSELs can significantly suppress the TDS [36, 37]. In addition to the optical feedback scheme, Hong et al. also experimentally demonstrated a broadband chaos in VCSELs subject to chaotic optical injection, continuous-wave (CW) optical injection, and self-feedback injection [38-40]. Besides, Quirce et al. experimentally observed that simultaneously combining the optical feedback and injection schemes in VCSELs can enhance the chaotic bandwidth. So far, however, the bandwidth of chaotic signals generated from VCSELs has only been tens gigahertz, which will constrict the rate of random number generation.

In 2009, Chan et al. numerically demonstrated the generation of broadband chaos in DFB lasers with strong modulation optical injection [41]. Herein, we experimentally demonstrate a broadband and no TDS chaos signal generation scheme based on a VCSEL with intensity modulation optical injection. In present works, by properly adjusting experiment parameters, a chaotic signal with a bandwidth above 20 GHz can be captured experimentally. Furthermore, we demonstrate a physical random number generation scheme based on the chaotic output from the aforementioned VCSEL. By adopting a simple multi-bit extraction method [42], we obtain 320 Gb/s random number sequences with verified randomness.

This paper is organized as follows. In Appendix B, we show the polarization-resolved intensities for the free-running VCSEL. In Appendix C, we display the key characteristics of our generated broadband chaos signal including the optical spectra, power spectra, time-delayed signal, intensity time series, and chaotic bandwidth. In Appendix D, we also exhibit the probability distribution of the decimal digitization levels when the number of extracted LSBs gradually augments.

* Corresponding author (email: nli@suda.edu.cn)

Appendix B Power-Current curve

In this section, we display the polarization-resolved intensities for the free-running VCSEL in Fig. B1. From this figure, we can see that the threshold current of the VCSEL is 2.15 mA. When 2.15 mA $< \mu <$ 3.05 mA, the Y-polarization (YP) mode is the dominant polarization mode, while the XP mode is suppressed. At $\mu = 3.05$, the polarization switching (PS) can be observed. When the drive current further increases, the XP mode evolves into the dominant polarization mode, and the YP mode is suppressed significantly.

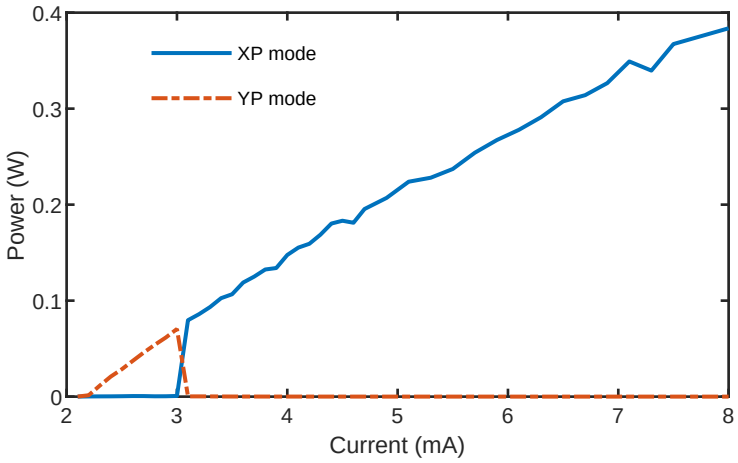

Figure B1 The polarization-resolved intensities of bump current μ for XP and YP modes of the free-running VCSEL.

Appendix C The characteristics of chaotic signals

In the experiment, the temperature of the VCSEL is fixed at 29°C and the wavelength of the TL is adjusted in real-time to form the frequency detuning f_i = f_{ML} - f_{SL} between the ML and the SL, where f_{ML} and f_{SL} stand for the center frequency of the free-running ML and the XP mode frequency of the VCSEL, respectively. The optical modulation depth, represented by the sideband-to-carrier ratio (SCR)[43], is 3 dB as shown in Fig. C1. To quantitatively investigate the chaotic characteristic, we calculate the chaotic bandwidth using the 80% standard bandwidth definition [44].

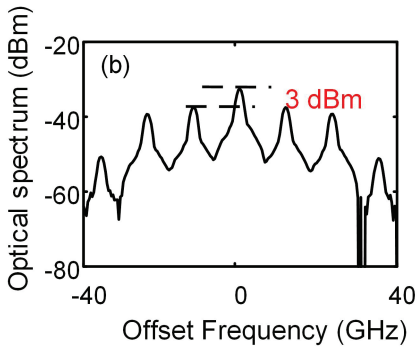

Figure C1 Optical spectra of IM input.

The autocorrelation function (ACF) [45] can be described as follows:

$$C(\Delta t) = \frac{\langle [I(t+\Delta t) - \langle I(t+\Delta t)\rangle][I(t) - \langle I(t)\rangle]\rangle}{\sqrt{\langle [I(t+\Delta t) - \langle I(t+\Delta t)\rangle]^2\rangle \langle [I(t) - \langle I(t)\rangle]^2\rangle}} \tag{C1}$$

where <> represents the average of the time series $I(t)$, Δt is the time shift. Moreover, the delay mutual information (DMI) [46]is defined as follows:

$$I = \sum_{I,I_\tau} p(I, I_\tau) \log[p(I, I_\tau)/p(I)p(I_\tau)] \tag{C2}$$

where $p(I)$ and $p(I_\tau)$ are respectively the probability density function of I, I_τ and $p(I, I_\tau)$ is the joint probability density function of (I, I_τ) .

Figure C2 shows the evolution of chaotic bandwidth under various injection frequency detuning f_i, where only maximum chaotic bandwidth is indicated for the given frequency detuning. Because the chaos is only found within a limited range of operating conditions, discrete data points are displayed in Fig. C3. Here, we first set the drive current μ = 5 mA (gray dot). As can be

seen when the absolute value of injection frequency detuning increases, the chaotic bandwidth is increased continuously for either positive or negative values. Furthermore, a larger chaotic bandwidth can be obtained in the case of negative frequency detuning by contrast with the case of positive frequency detuning. Similar results are seen with a higher drive current μ = 8 mA. In Table C1, we list some typical chaotic generation schemes based on VCSELs. Compared with other schemes, our proposed scheme at least doubles the chaotic bandwidth. Besides, we also try to further enlarge chaotic bandwidth by increasing the drive current or injection frequency detuning. However, we find that when the drive current exceeds 8 mA, the output power of the VCSEL remains almost constant at 0.38 mW, which is significantly different from the DFB laser. Fortunately, when the absolute value of injection frequency detuning further increases, the high-frequency component in the microwave power spectrum can be upraised away from the noise floor. Nevertheless, limited by the bandwidth of PD, a larger chaotic bandwidth is not measured.

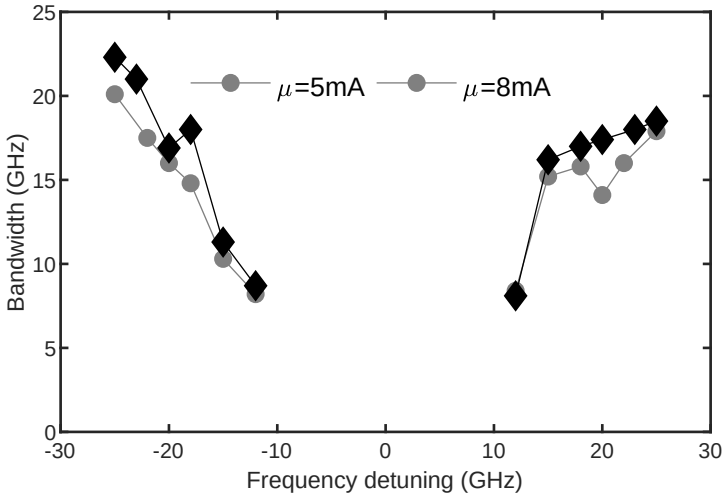

Figure C2 Chaos bandwidth as a function of the injection frequency detuning.

Figure C3 displays the time series and the corresponding probability density function from experimentally achieved chaotic signals, where the injection parameters and modulation parameters are (ξ_i, f_i) = (1, 26 GHz) and f_m = 14 GHz. One can see that the time series presents a noise-like fluctuation, and symmetrical amplitude distribution by contrast with the Gaussian fitting (blue curve).

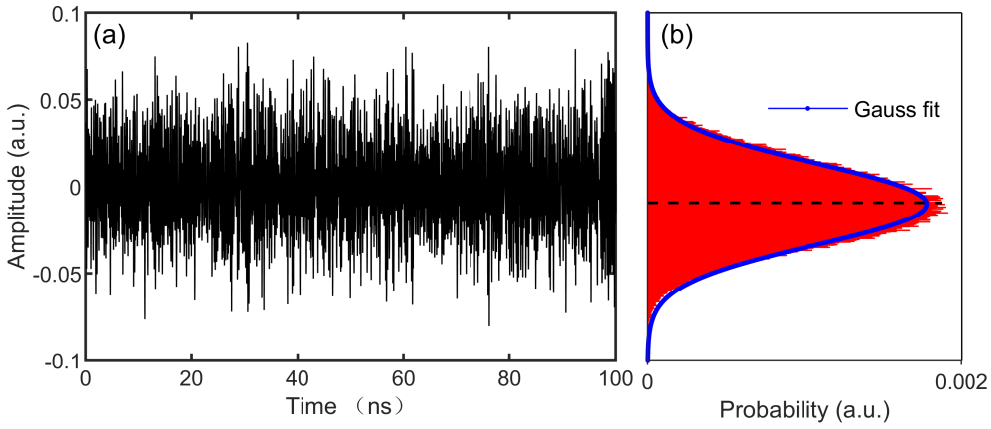

Figure C3 (a) Time trace and (b) probability density distribution.

Appendix D Random number generation

In Fig. D1, we exhibit the probability distribution of the decimal digitization levels when the number of extracted LSBs gradually augments. Concretely, when 7-LSBs are retained, the probability distribution is described in Fig. D1(g), in which an obvious non-uniform distribution can be observed. When further discarding several of the most significant bits (MSB), as shown in Figs. D1(e) and D1(f) where we retain 5-LSBs and 6-LSBs, the uniformity is markedly improved. When the LSB decreases to 4, a uniformity and flat probability distribution can be obtained as shown in Fig. D1(d), which is one of the most important prerequisites for producing unbiased and reliable random bits.

Table C1 Comparisons of chaos bandwidth based on VCSELs

Method	Bandwidth	Reference
Orthogonal optical injection and optical feedback	4.47 GHz	[47]
CW injected chaotic VCSELs	4.5 GHz	[38]
Chaotic injected into a CW VCSEL	9.3 GHz	[38]
Chaotic signal injected into a chaotic VCSEL	2.7 GHz	[38]
Additional fiber ring resonator	11 GHz	[35]
A Chaotic VCSEL mutually coupled with a CW VCSEL	∼14 GHz	[40]
A CW VCSEL mutually coupled with another CW VCSEL	∼13 GHz	[40]
VCSEL with intensity modulation optical injection	>20 GHz	This work

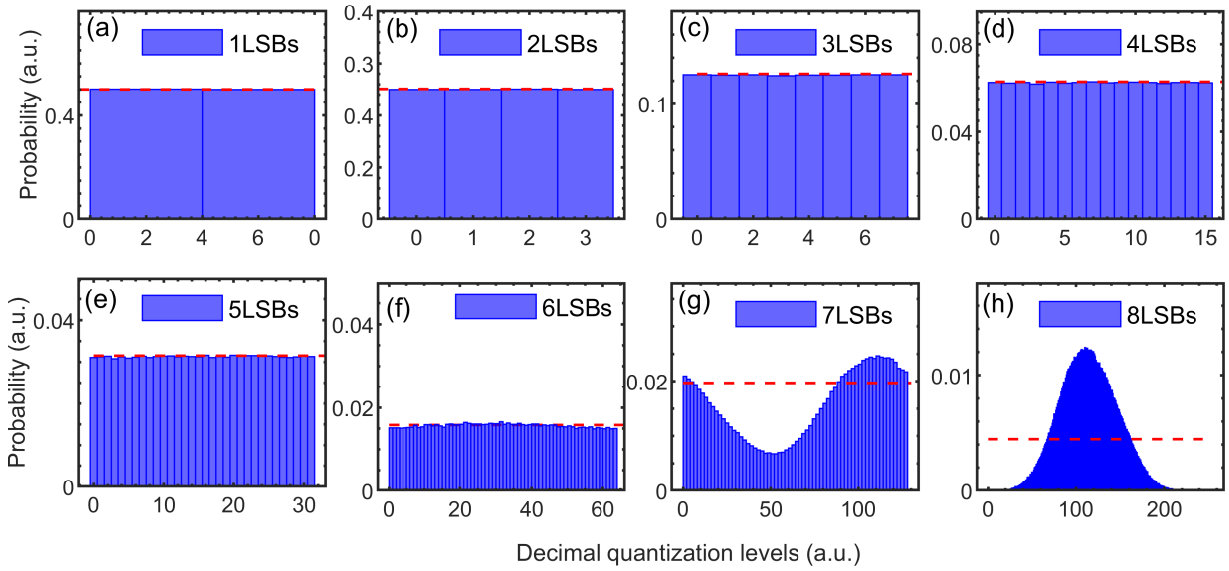

Figure D1 Probability distribution histogram of the decimal digitization levels for (a) 1LSBs, (b) 2LSBs, (c) 3LSBs, (d) 4LSBs, (e) 5LSBs, (f) 6LSBs, (g) 7LSBs, (h) 8LSBs retained from each 8-bit sample. Standard probability values of theoretical statistics (red dotted lines).

References

1 Gallager R G, Principles of digital communication. Cambridge University Press: 2008;
2 Asmussen S, Glynn P W, Stochastic simulation: algorithms and analysis. Springer: 2007; Vol. 57
3 Stinson D R, Cryptography: theory and practice. Chapman and Hall/CRC: 2005;
4 Wang J, Cui K, Luo C, et al. Design of a high-repetition rate photon source in a quantum key distribution system. Sci. China Inf. Sci., 2013, 56: 092305-092305
5 Huang Y, Zhang F, Liu Z, et al. Pseudorandom number generator based on supersingular elliptic curve isogenies. Sci. China Inf. Sci., 2022, 65: 159101
6 Ge Z, Hao T, Capmany J, et al. Broadband random optoelectronic oscillator. Nat. Commun., 2020, 11: 1-8
7 Kanter I, Aviad Y, Reidler I, et al. An optical ultrafast random bit generator. Nat. Photonics, 2010, 4: 58-61
8 Ma C-G, Xiao J-L, Xiao Z-X, et al. Chaotic microlasers caused by internal mode interaction for random number generation. Light-SCI. Appl., 2022, 11: 187
9 Li N, Kim B, Chizhevsky V N, et al. Two approaches for ultrafast random bit generation based on the chaotic dynamics of a semiconductor laser. Opt. Express, 2014, 22: 6634-46
10 Valle-Mi?on M., Quirce A., Valle A., et al., Quantum random number generator based on polarization switching in gain-switched VCSELs. Opt. Continuum, 2022, 1: 2156-2166.
11 Abell n C., Amaya W., Jofre M., et al., Ultra-fast quantum randomness generation by accelerated phase diffusion in a pulsed laser diode. Opt. Express, 2014, 22(2), 1645-1654.
12 Uchida A, Amano K, Inoue M, et al. Fast physical random bit generation with chaotic semiconductor lasers. Nat. Photonics, 2008, 2: 728-732
13 Lin F Y, Liu J M. Chaotic lidar. IEEE J. Sel. Top. Quantum Electron., 2004, 10: 991-997
14 Jiang L, Feng J, Yan L, et al. Chaotic optical communications at 56 Gbit/s over 100-km fiber transmission based on a chaos generation model driven by long short-term memory networks. Opt. Lett., 2022, 47: 2382-2385
15 Jiang N, Pan W, Luo B, et al. Simultaneous unidirectional and bidirectional chaos-based optical communication using hybrid coupling semiconductor lasers. Sci. China Inf. Sci., 2012, 57: 1-11
16 Zhao A, Jiang N, Chang C, et al. Generation and synchronization of wideband chaos in semiconductor lasers subject to

constant-amplitude self-phase-modulated optical injection. Opt. Express, 2020, 28: 13292-13298
17 Bouchez G, Uy C-H, Macias B, et al. Wideband chaos from a laser diode with phase-conjugate feedback. Opt. Lett., 2019, 44: 975-978
18 Han Y, Xiang S, Wang Y, et al. Generation of multi-channel chaotic signals with time delay signature concealment and ultrafast photonic decision making based on a globally-coupled semiconductor laser network. Photonics Res., 2020, 8: 1792-1799
19 Li N, Nguimdo R M, Locquet A, et al. Enhancing optical-feedback-induced chaotic dynamics in semiconductor ring lasers via optical injection. Nonlinear Dynam., 2018, 92: 315-324
20 Nguimdo R M, Verschaffelt G, Danckaert J, et al. Loss of time-delay signature in chaotic semiconductor ring lasers. 2012, 37: 2541-2543
21 Lin H, Hong Y, Ourari S, et al. Quantum dot lasers subject to polarization-rotated optical feedback. IEEE J. Quantum. Electron., 2020, 56: 2000308
22 Li J-C, Xiao J-L, Yang Y-D, et al. Nonlinear dynamics in a circular-sided square microcavity laser. Photonics Res., 2023, 11: A97-A106
23 Deng Y, Fan Z-F, Zhao B-B, et al. Mid-infrared hyperchaos of interband cascade lasers. Light-Sci. Appl., 2022, 11: 7
24 Liu W, Huang Y, Sun Y, et al. Broadband and flat millimeter-wave noise source based on the heterodyne of two Fabry Perot lasers. Opt. Lett., 2021, 47:
25 Guo Y, Liu W, Huang Y, et al. Fast physical random bit generation using a millimeter-wave white noise source. Opt. Express, 2022, 30: 541-544
26 Li N Q, Susanto H, Cemlyn B, et al. Secure communication systems based on chaos in optically pumped spin-VCSELs. Opt. Lett., 2017, 42: 3494-3497
27 Virte M, Panajotov K, Thienpont H, et al. Deterministic polarization chaos from a laser diode. Nat. Photonics, 2012, 7: 60-65
28 Alharthi S S, Orchard J, Clarke E, et al. 1300 nm optically pumped quantum dot spin vertical external-cavity surface-emitting laser. Appl. Phys. Lett., 2015, 107: 151109
29 Adams M J, Alexandropoulos D. Analysis of quantum-dot spin-VCSELs. IEEE Photonics J., 2012, 4: 1124-1132
30 Li N Q, Susanto H, Cemlyn B, et al. Stability and bifurcation analysis of spin-polarized vertical-cavity surface-emitting lasers. Phys. Rev. A, 2017, 96: 013840
31 Schires K, Al-Seyab R, Hurtado A, et al. Optically-pumped dilute nitride spin-VCSEL. Opt. Express, 2012, 20: 3550-3555
32 Priyadarshi S, Yanhua H, Pierce I, et al. Experimental investigations of time-delay signature concealment in chaotic external cavity VCSELs subject to variable optical polarization angle of feedback. IEEE J. Sel. Top. Quantum Electron., 2013, 19: 1700707-1700707
33 Hong Y, Spencer P S, Shore K A. Wideband chaos with time-delay concealment in vertical-cavity surface-emitting lasers with optical feedback and injection. IEEE J. Quantum. Electron., 2014, 50: 236-242
34 Lin H, Hong Y, Shore K A. Experimental study of time-delay signatures in vertical-cavity surface-emitting lasers subject to double-cavity polarization-rotated optical feedback. J. Lightwave. Technol., 2014, 32: 1829-1836
35 Hong Y, Chen X, Spencer P S, et al. Enhanced flat broadband optical chaos using low-cost VCSEL and fiber ring resonator. IEEE J. Quantum. Electron., 2015, 51: 1200106
36 Zhong Z Q, Wu Z M, Xia G Q. Experimental investigation on the time-delay signature of chaotic output from a 1550 nm VCSEL subject to FBG feedback. Photonics Res., 2016, 5: 6-10
37 Cai W, Xiang S, Cao X, et al. Experimental investigation of the time-delay signature of chaotic output and dual-channel physical random bit generation in 1550 nm mutually coupled VCSELs with common FBG filtered feedback. Appl Opt, 2020, 59: 4583-4588
38 Hong Y, Spencer P S, Shore K A. Flat broadband chaos in vertical-cavity surface-emitting lasers subject to chaotic optical injection. IEEE J. Quantum. Electron., 2012, 48: 1536-1541
39 Hong Y, Paul S. Spencer, Shore a K A. Enhancement of chaotic signal bandwidth in vertical-cavity surface-emitting lasers with optical injection. J. Opt. Soc. Am. B, 2012, 29: 415-419
40 Huang Y. Flat broadband chaos in mutually coupled vertical-cavity surface-emitting lasers. IEEE J. Sel. Top. Quantum Electron., 2015, 21: 652-658
41 Chan S-C, Tang W K, Chaos. Chaotic dynamics of laser diodes with strongly modulated optical injection. International Journal of Bifurcation, 2009, 19: 3417-3424
42 Reidler I, Aviad Y, Rosenbluh M, et al. Ultrahigh-speed random number generation based on a chaotic semiconductor laser. Phys. Rev. Lett., 2009, 103: 024102
43 Tseng C-H, Lin C-T, Hwang S-K. V- and W-band microwave generation and modulation using semiconductor lasers at period-one nonlinear dynamics. Opt. Lett., 2020, 45: 6819-6822
44 Lin F-Y, Chao Y-K, Wu T-C. Effective bandwidths of broadband chaotic signals. IEEE J. Quantum. Electron., 2012, 48: 1010-1014
45 Jiang P, Zhou P, Li N, et al. Characterizing the chaotic dynamics of a semiconductor nanolaser subjected to FBG feedback. Opt. Express, 2021, 29: 17815-17830
46 Rontani D, Locquet A, Sciamanna M, et al. Loss of time-delay signature in the chaotic output of a semiconductor laser with optical feedback. Opt. Lett., 2007, 32: 2960-2962
47 Quirce A, Valle A, Thienpont H, et al. Enhancement of chaos bandwidth in VCSELs induced by simultaneous orthogonal optical injection and optical feedback. IEEE J. Quantum. Electron., 2016, 52: 2400609